

Early CT manifestations and short-term evolution of coronavirus disease-2019

Wei Wei (✉ weiweill@126.com)

Anhui Provincial Hospital <https://orcid.org/0000-0003-4097-1592>

Wen Xiao Hu

Anhui Provincial Hospital

Fu Wei Lv

Anhui Provincial Hospital

Research Article

Keywords: Coronavirus, Disease, X-rays, Tomography

Posted Date: March 30th, 2020

DOI: <https://doi.org/10.21203/rs.3.rs-19012/v1>

License:  This work is licensed under a Creative Commons Attribution 4.0 International License.

[Read Full License](#)

Abstract

Objectives: This study explored the features of coronavirus disease-2019 (COVID-19) with the aim of improving clinical diagnosis.

Methods: We retrospectively analyzed the clinical and CT data of 85 patients with COVID-19 who were diagnosed between January 20, 2020 and February 20, 2020. The imaging findings, clinical and laboratory data were evaluated.

Results: Of the 85 patients, five had mild symptoms, 60 had moderate symptoms, and 20 had severe symptoms. Sixty-nine patients had direct or indirect contact history, while 16 patients (19%) had no obvious epidemiological history. Eighty-five patients had prominent respiratory symptoms, while 70 patients (82%) had moderate to low fever. There were no obvious lung abnormalities in CT images of patients with mild symptoms. Common chest CT manifestations in patients with moderate or severe symptoms were ground glass opacity (GGO) (16%); GGO combined with grid (39%) or consolidation (32%); and air bronchogram sign (13%). In these patients, lesions were mostly distributed in the lower lobes of the lungs, and most were located in the periphery; pleural effusion was rare. Within 3 days after onset, GGO (23%) and GGO combined with grid (45%) were the most common manifestations in CT images; GGO combined with grid (35%) and/or consolidation (41%) were the main manifestations in CT images at 5–10 days after onset.

Conclusions: Common CT manifestations of COVID-19 were GGO alone and GGO combined with grid and/or consolidation. Short-term increases in ranges of lesions or consolidation areas may indicate disease aggravation.

Introduction

A novel coronavirus was discovered in Wuhan, Hubei, China in December 2019^{1,2}. It was named coronavirus disease-2019 (COVID-19) by the World Health Organization on February 11, 2020. The incubation period of the virus after infection is generally 3–7 days (up to 14 days), and it is highly infectious^{3,4}. The outbreak initially occurred in Wuhan, then spread to many cities in China. The First Affiliated Hospital of University of Science and Technology of China (Anhui Provincial Hospital) and the Affiliated Infectious Disease Hospital have been designated for the treatment of patients with new coronavirus infection in Anhui Province. Between January 2020 and February 2020, these hospitals admitted 85 patients with confirmed COVID-19 infection. This retrospective study was performed to analyze the clinical and imaging data of these 85 patients, with the aim of exploring the early imaging symptoms and short-term evolution of COVID-19, which will aid in clinical diagnosis.

Materials And Methods

Patients and ethical approval

Our institutional review board (IRB) waived written informed consent for this retrospective study, that evaluated de-identified data and involved no potential risk to patients. To avert any potential breach of confidentiality, no link between the patients and the researchers was made available.

For the period from January 20, 2020 to February 20, 2020, patients were included if they met the following criteria: (1) they exhibited positive finding for the 2019-nCoV nucleic acids; (2) they had undergone chest thin-layer computed tomography (CT) examination during initial diagnosis (within 3 days of onset) and at the short-term follow-up visit (5–10 days after the initial CT examination). Patients were excluded from this study if they exhibited pneumonia caused by other common bacterial or viral pathogens.

Image acquisition

CT imaging and high-resolution reconstruction were performed for all patients. For each patient, the first CT scan was performed within 3 days after disease onset; the interval between the first CT scan and the follow-up visit was 5–10 days (generally within 7 days). All CT examinations were performed with a 128-slice CT detector (NeuViz128) without contrast agent. Scanning parameters were as follows: tube potential, 120 kV; tube current, 150 mA; iterative reconstruction technology; detector collimation width, 128 × 1.25 mm; rotation time, 0.8 s; scanning layer thickness, 5 mm; pitch, 1.2; matrix, 512 × 512; and breath holding when fully aspirated. Reconstruction was performed using a high-resolution algorithm with a layer thickness of 1.25 mm. Two windows were used: a mediastinal window with a width of 350 HU and level of 40 HU; and a lung window with a width of 1500 HU and level of -700 HU. Two radiologists with more than 10 years of experience in chest imaging diagnosis independently read these images; disagreements were resolved by discussion.

CT images were used to evaluate the types and distribution of lesions. The types of lesions were as follows: □ pure GGO; □ GGO with interlobular septal thickening or intralobular network; □ GGO with consolidation; □ air bronchogram; □ pleural effusion. The distributions of lesions were as follows: □ by lung segment (number of involved lung segments was regarded as the number of lesions); □ on axial CT images, the outer third of the lung was defined as peripheral, while the remaining portion was defined as central.

Statistical analysis

Statistical analysis was performed using SPSS Statistics, version 20.0 (IBM Corp.). Data are shown as mean ± standard deviation. The proportions of the types of lesions in the first CT and short-term follow-up CT images were compared by Pearson χ^2 tests. Differences with $P < 0.05$ were considered statistically significant.

Results

Patient characteristics

Eighty-five patients with confirmed COVID-19 infection were included in this study. The clinical characteristics and laboratory results of these 85 patients are shown in Table 1. Of the 85 patients, 34 were women (40%) and 51 were boys or men (60%). The mean age was 45.35 ± 16.91 years.

Epidemiological history

Twenty-six patients had traveled to or resided in Wuhan and surrounding areas within 14 days before onset. Twenty-four patients had been in contact with patients who had confirmed COVID-19 infection within 14 days before onset. Nineteen patients had been exposed to patients with confirmed COVID-19 infection from Wuhan and surrounding areas, or to patients from other areas with confirmed infection who exhibited fever or respiratory symptoms. Sixteen patients had no clear epidemiological history.

The main clinical symptoms were fever in 76 patients, asthenia in 25 patients, and diarrhea in three patients. All patients had different respiratory symptoms: cough, sputum, and/or chest tightness. Laboratory examinations revealed that, in most patients, leukocyte count was normal (66/85, 78%) and neutrophil count was normal (81/85, 95%); however, lymphocyte count was low (42/85, 49%). C-reactive protein levels were elevated in 64/85 patients (75%). Moreover, 37 patients (44%) had low CD4+ cell count, ranging from 98–302 cells/ μ L.

In accordance with guidelines for the diagnosis and treatment of patients with COVID-19 infected pneumonia (trial sixth edition)⁵, clinical classifications were mild, moderate, severe, and critical. In our study, the respiratory tract samples of 85 patients were positive for 2019-nCoV nucleic acid. The clinical classifications were as follows: five patients (6%), including two women, had no obvious abnormality in the initial or follow-up lung CT (i.e., mild disease); they were 4–34 years of age at disease onset (mean age, 20.4 ± 11.17 years). Sixty patients (71%), including 29 women, exhibited moderate disease; they were 21–63 years of age at disease onset (mean age, 43.90 ± 13.69 years). Twenty patients (23%), including three women, exhibited severe disease; they were 21–91 years of age at disease onset (mean age, 56.00 ± 19.27 years). Most of the patients had underlying diseases: two had mitral stenosis, two had cerebral infarction, three had diabetes, and five had hypertension. There were no patients with critical disease in this study; all patients recovered and were discharged.

CT manifestations

Five patients had no obvious abnormality in the initial or follow-up lung CT. The distribution and morphology of pulmonary lesions in other 80 patients, as determined by CT, are shown in Tables 2 and 3. In the initial CT images, there were 715 segments involving 80 patients. Eleven patients had fewer than five segments involved; 39 patients had 5–10 segments involved; 30 patients had more than 10 segments involved; and four patients had all segments of both lungs involved. In 73 of 80 (91%) patients, 421 of 715 (59%) lesions were distributed in the lower lobes of both lungs; in 77 of 80 (96%) patients, the lesions were distributed around the lung. The morphologies and densities of the lesions are depicted in Figures 1 and 2. GGO (nodular, patchy, and lamellar GGO) was observed in 67 of 80 (84%) patients; GGO with interlobular septal thickening was observed in 62 of 80 (78%) patients; GGO with consolidation was

observed in 20 of 80 (25%) patients; air bronchogram was observed in 14 of 80 (18%) patients; and pleural effusion was observed in four of 80 patients.

In the short-term follow-up CT images, there were 940 pulmonary segments involving 80 patients. Six patients had fewer than five lung segments involved; 42 patients had 5–10 lung segments involved; 32 patients had more than 10 lung segments involved; and seven patients had all segments of both lungs involved. In 73 of 80 (91%) patients, 569 of 940 (60%) lesions were distributed in the lower lobes of both lungs; in 77 of 80 (96%) patients, the lesions were distributed around the lung. The morphologies and densities of the lesions were as follows: GGO was observed in 26 of 80 (33%) patients; GGO with interlobular septal thickening was observed in 72 of 80 (90%) patients; GGO with consolidation was observed in 47 of 80 (59%) patients; air bronchogram was observed in 31 of 80 (39%) patients; and pleural effusion was observed in three of 80 patients.

Comparison of images between patients with moderate disease and those with severe disease revealed the following findings. First, 238 lung segments (mean, 12 segments/patient) were involved in initial CT examinations of 20 patients with severe disease, while 324 lung segments (mean, 16 segments/patient) were involved in short-term follow-up CT examinations; in contrast, 477 lung segments (mean, eight segments/patient) were involved in initial CT examinations of 60 patients with moderate disease, while 616 lung segments (mean, 10 segments/patient) were involved in short-term follow-up CT examinations. Second, all patients in whom all lung segments of both lungs were involved during the initial and follow-up CT examinations exhibited severe disease. Third, CT images of 20 patients with severe disease revealed that the scope of lesions was significantly enlarged and multiple consolidations were present (Figure 3).

Crosstabulation in SPSS 20.0 was used to analyze pathological changes in the initial and follow-up CT images. We found that the proportion of images with pathological changes was significantly different between CT images taken before and after diagnosis (Pearson $\chi^2 = 95.623$, $P < 0.001$). Moreover, the proportion of images with pure GGO decreased on follow-up CT images, whereas there were increased proportions of images with internal grid opacity and solid area (Table 1).

Discussion

The currently prevalent COVID-19 is caused by 2019-nCoV infection. COVID-19 was first prevalent in Wuhan, then gradually spread to most cities in China. Most of the patients in our hospital had epidemiological history (69/85, 81%); however, the proportion of patients without obvious epidemiological history was considerably greater (16/85, 19%) than in previous reports by Huang et al⁶. Patients without obvious epidemiological history were mostly unemployed, engaged in catering or retain work, with an undefined scope of activity and contact population; these factors may have increased their susceptibility.

Thus far, there are few characteristic symptoms of COVID-19; common symptoms are fever, cough, and sputum, but high fever is rare^{6,7}. In this study, only six of 85 patients (7%) had high fever, while intermediate/low fevers were common (70/85 patients, 82%); 9 patients (11%) had no obvious fever. The clinical manifestations observed in this study suggest that the use of fever as an important aspect of clinical diagnosis may lead to missed diagnosis in some patients. Patients with COVID-19 may exhibit symptoms of diarrhea⁸, but only three patients in this study exhibited such symptoms.

During initial CT imaging, the early imaging characteristics of patients with moderate and severe disease were mainly GGO and GGO combined with fine grid opacity. Patients with severe disease exhibited diffuse lesion distribution; in four patients, all lung segments of both lungs were involved in initial CT images. Lesions were mostly observed in the peripheral zone of the lung field, particularly the lower lobe (approximately 60% of lesions). During short term follow-up CT imaging, important changes were observed: there were smaller ground glass opacity lesions in patients with moderate disease, and some of these lesions were resolved. Furthermore, new GGO lesions appeared in some lung areas in patients with severe disease; in three patients, the ground glass opacity rapidly progressed to involve all lung segments of both lungs. Grid opacity and consolidation appeared in most GGO lesions; the air bronchogram incidence was also higher than it had been during the initial examination. In both initial and follow-up CT imaging examinations, there were high incidences of GGO and GGO combined with grid or consolidation; these findings indicated progression of pulmonary interstitial changes, consistent with the results reported by Song et al.⁹. Therefore, during imaging diagnosis, COVID-19 should be differentiated from other interstitial changes caused by viral pneumonia, mycoplasma pneumonia, and non-infectious diseases¹⁰⁻¹².

In this study, our results showed that the diagnosis of COVID-19 is not limited to individuals with a clear epidemiological history, and that patients' occupations may affect their activities and potential contact with infected individuals. Furthermore, patients with COVID-19 may not exhibit fever. Notably, CT findings in patients with COVID-19 are consistent with the manifestations in patients with viral pneumonia, but the distribution of lesions is largely limited to the lung field and two lower lobes. This study showed that the severity of disease can be determined by notable changes in follow-up images, such as enlarged lesion scope and increased consolidation. In addition, lesions progress rapidly in patients with severe COVID-19; COVID-19 is likely to occur in the elderly with multiple underlying diseases, similar to other types of viral pneumonia^{13,14}.

There were some limitations in this study. First, the sample size was relatively small, so in-depth analysis could not be performed. Second, because of the absence of complete and dynamic image data, no analysis of the final imaging outcome of the disease was possible. Third, no comparative analysis of imaging and histopathology findings could be performed.

Conclusion

In this study, the common chest CT manifestations of patients with COVID-19 were GGO mainly distributed around the lung field, as well as GGO combined with grid or consolidation. In addition, our findings showed that chest CT images can be used for rapid and effective imaging diagnosis of COVID-19 and evaluation of disease progression. Finally, the combination of epidemiological history, clinical manifestations, and imaging data can aid in diagnosis of patients with suspected COVID-19; however, the nucleic acid test remains the gold standard for diagnosis.

Declarations

Ethical Approval and Consent to participate

Our institutional review board (IRB) waived written informed consent for this retrospective study, that evaluated de-identified data and involved no potential risk to patients. To avert any potential breach of confidentiality, no link between the patients and the researchers was made available.

Consent for publication

Not applicable.

Availability of data and materials

Data sharing is not applicable to this article as no datasets were generated or analysed during the current study.

Competing interests

The authors declared that they have no conflicts of interest to this work. We declare that we do not have any commercial or associative interest that represents a conflict of interest in connection with the work submitted.

Funding

The authors state that this work has not received any funding.

Authors' contributions

Wei wei: Data curation, Writing - original draft. Xiao-wen Hu: Data curation. Wei-Fu Lv: Conceptualization, Methodology.

Acknowledgements

None.

References

1. WHO, Novel Coronavirus – China, Jan 12 (2020) (Accessed Jan 19, 2020),
<http://www.who.int/csr/don/12-january-2020-novel-coronavirus-china/en/>.
2. N.S. Chen, M. Zhou, X. Dong, J.M. Qu, F.Y. Gong, Y. Han, Y. Qiu, J.L. Wang, Y. Liu, Y. Wei, J.A. Xia, T. Yu, X.X. Zhang, L. Zhang, Epidemiological and clinical characteristics of 99 cases of 2019 novel coronavirus pneumonia in Wuhan, China: a descriptive study, *Lancet* 395 (10223) (2020) 507–513, [https://doi.org/10.1016/S0140-6736\(20\)30211-7](https://doi.org/10.1016/S0140-6736(20)30211-7).
3. Chan JF, Yuan SF, Kok KH, Wang KK, Chu H, Yang J, et al. A familial cluster of pneumonia associated with the 2019 novel coronavirus indicating person-to-person transmission: a study of a family cluster. *Lancet*, 395(10223), (2020)514-523. [https://doi.org/10.1016/S0140-6736\(20\)30154-9](https://doi.org/10.1016/S0140-6736(20)30154-9).
4. A. Patel, D.B. Jernigan, 2019-nCoV CDC Response Team, Initial public health response and interim clinical guidance for the 2019 novel coronavirus outbreak - United States, December 31, 2019–February 4, 2020, *Am. J. Transplant.* 20 (3) (2020)889–895, <https://doi.org/10.1111/ajt.15805>.
5. General Office of National Health Committee. Office of State Administration of Traditional Chinese Medicine. Notice on the issuance of a programme for the diagnosis and treatment of novel coronavirus (2019-nCoV) infected pneumonia (trial sixth edition) (2020-02-18) [EB/OL].
<http://yzs.satcm.gov.cn/zhengcewenjian/2020-02-19/13221.html>.
6. C.L. Huang, Y.M. Wang, X.W. Li, L.L. Ren, J.P. Zhao, Y. Hu, Clinical features of patients infected with 2019 novel coronavirus in Wuhan, China, *Lancet* 395 (10223) (2020) 497–506, [https://doi.org/10.1016/S0140-6736\(20\)30183-5](https://doi.org/10.1016/S0140-6736(20)30183-5).
7. Zhu N, Zhang D, Wang W, Li X, Yang B, Song J, et al. A novel coronavirus from patients with pneumonia in China, 2019[J]. *N Engl J Med*, 2020, doi: 10.1056/NEJMoa2001017.
8. Wang WG, Hu H, Song L, Gong XM, Qu YJ, Lu ZY. Image of pulmonary and diagnosis of atypical novel coronavirus (2019-nCoV) infected pneumonia: case series of 14 patients[J]. *New Med*, 2020, 30(1): 7-9.
9. Song FX, Shi NN, Shan F, Zhang ZY, Shen J, Lu HZ, et al. Emerging Coronavirus 2019-nCoV Pneumonia[J]. *Radiology*. doi:10.1148/radiol.2020200274.
10. Wong KT, Antonio GE, Hui DS, Lee N, Yuen EH, Wu A, et al. Thin-section CT of severe acute respiratory syndrome: evaluation of 73 patients exposed to or with the disease[J]. *Radiology*, 2003,228(2): 395-400.
11. Koo HJ, Lim S, Choe J, Choi SH, Sung H, Do KH. Radiographic and CT Features of Viral Pneumonia[J]. *Radiographics*, 2018,38(3):719-739.
12. Ooi GC, Khong PL, Müller NL, Yiu WC, Zhou LJ, Ho JC, et al. Severe acute respiratory syndrome: temporal lung changes at thin-section CT in 30 patients[J]. *Radiology*, 2004, 230(3):836-44.
13. Li H, Weng H, Lan C, Zhang H, Wang X, Pan J, et al. Comparison of patients with avian influenza A (H7N9) and influenza A (H1N1) complicated by acute respiratory distress syndrome[J]. *Medicine*, 2018,97(12): e194.
14. Wang Q, Zhang Z, Shi Y, Jiang Y. Emerging H7N9 influenza A (novel reassortant avian-origin) pneumonia: radiologic findings[J]. *Radiology*, 2013,268(3):882-889.

Tables

Table 1. Epidemiological history and clinical data of 85 confirmed patients

	Characteristics	Number of cases	Percentage
Epidemiological history	1. History of travel or residence in Wuhan and surrounding areas	26	31%
	2. History of exposure to new coronavirus infections	24	28%
	3.Exposed to patients with fever or respiratory symptoms from Wuhan and surrounding areas, or from areas with case reports	19	22%
	4. No clear epidemiological history	16	19%
Gender	Male	51	60%
	Female	34	40%
Symptoms	No fever	9	11%
	Fever	37	44%
		33	38%
		6	7%
	Fatigue	25	29%
	Cough, expectoration and / or chest tightness	85	100%
Lab tests	White blood cell count	Normal	78%
		Decreased	16%
		Increased	6%
	Reduced lymphocyte count	42	49%
	Reduced CD4+ cell count	37	44%

Table 2. First and follow-up CT scans of 60 moderate and 20 severe NCP patients showed lung involvement

		First CT		Follow-up CT	
		Moderate	Severe	Moderate	Severe
		(60 cases)	(20 cases)	(60 cases)	(20 cases)
Superior lobe of left lung	Apical-posterior segment	31	14	31	17
	Anterior segment	18	5	18	12
	Superior lingular segment	24	7	24	14
	Inferior lingular segment	30	5	30	15
Superior lobe of right lung	Apical segment	22	6	26	17
	Anterior segment	20	7	21	16
	Posterior segment	30	12	32	18
Middle lobe of right lung	Medial basal segment	18	7	20	19
	Lateral segment	22	16	22	19
Inferior lobe of left lung	Superior segment	30	20	55	20
	Anterior basal segment	23	17	40	20
	Lateral basal segment	30	20	35	20
Inferior lobe of right lung	Posterior segment	38	19	49	20
	Superior segment	29	18	42	18
	Anterior basal segment	21	13	39	20
	Medial basal segment	22	14	41	19
	Lateral basal segment	28	18	37	20
	Posterior basal segment	41	20	54	20
Total		477	238	616	324
		715		940	

Table 3. First and follow-up CT showed the morphology and composition ratio of NCP lesions

	First CT	Follow-up CT	Total
GGO	164 23%	102 11%	266 16%
GGO+Grid	320 45%	330 35%	650 39%
GGO+consolidation	152 21%	382 41%	435 32%
Air bronchogram	79 11%	126 13%	205 13%
Total	715	940	1655
Pearson χ^2 =		95.623	
<i>p</i>		0.000	

Figures



Figure 2

A 67-year-old man presented with a 3-day history of fever, cough, and sputum. Approximately 2 weeks prior, he had been in contact with patients with COVID-2019. On the third day after disease onset, CT imaging revealed GGO with fine grid in the posterior segment of the left upper lobe tip, as well as pure GGO in the posterior segment of the right upper lobe and dorsal segment of the left lower lobe.

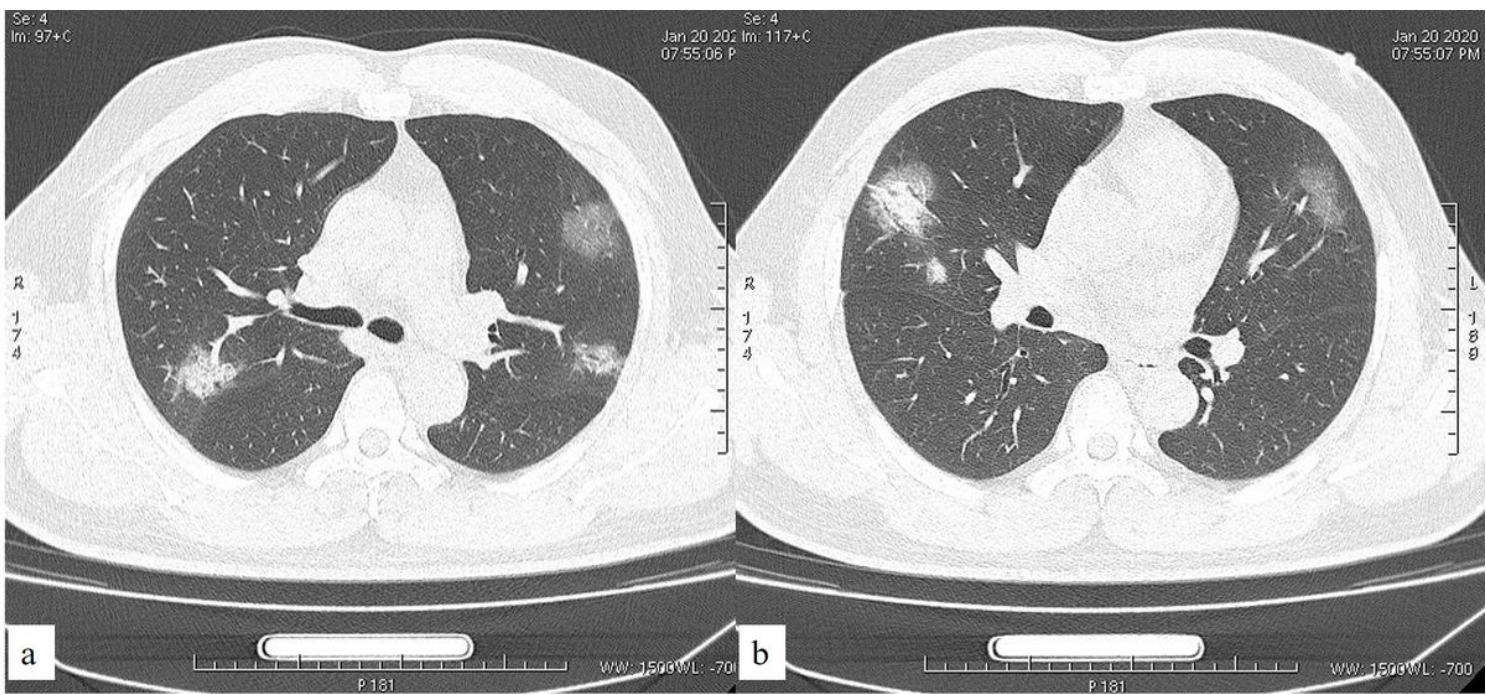


Figure 4

A 49-year-old man presented with a 3-day history of fever, cough, and muscle aches. He had traveled to Wuhan within 2 weeks before the onset of disease. On the third day after disease onset, CT imaging revealed GGO with consolidation in the posterior and lateral segments of the right upper lobe, as well as air bronchogram sign in the middle lobe lesions, and pure GGO in the left upper lobe.

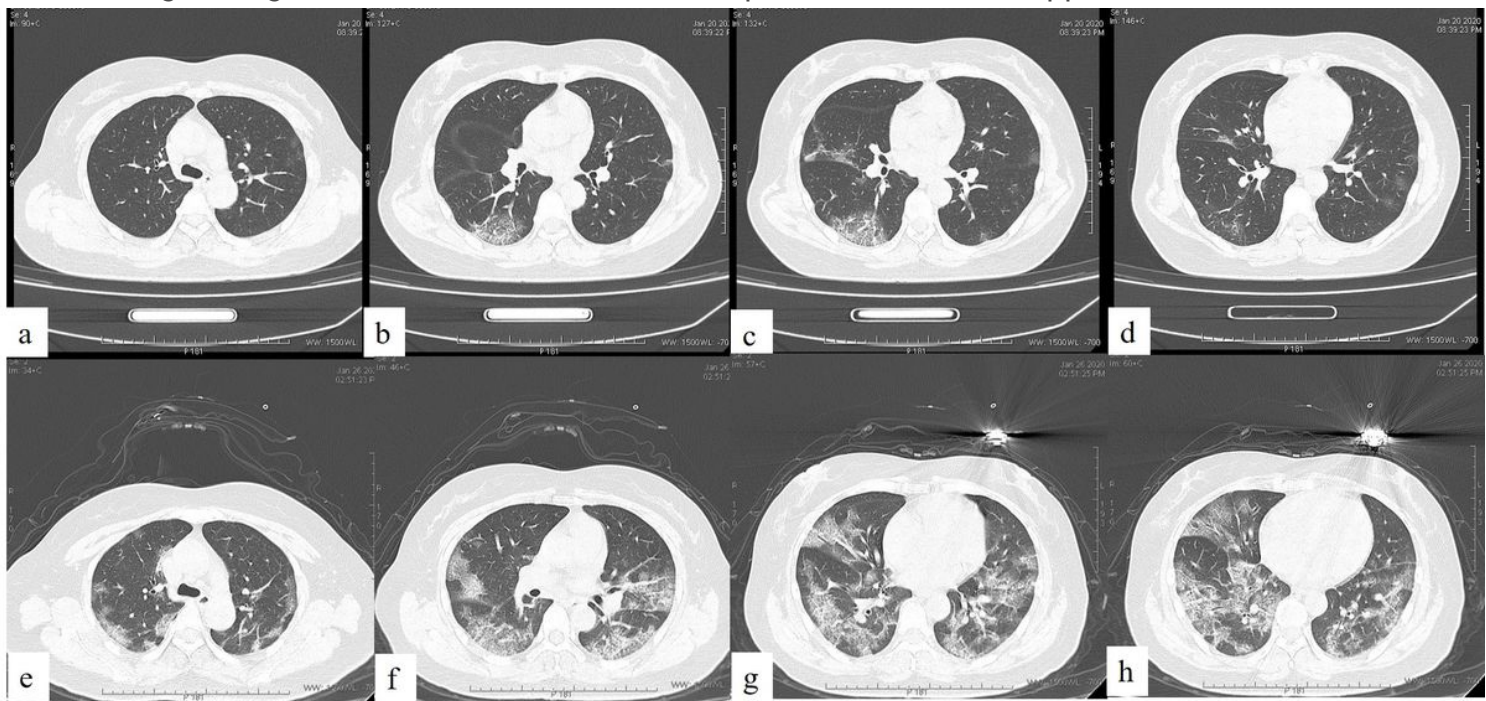


Figure 6

A 47-year-old woman presented with a 3-day history of fever, headache, and chest pain. Her husband had traveled to Wuhan for business on January 9, 2020. On the third day after disease onset, CT imaging (A–D) revealed scattered GGO under the left lung pleura, as well as ground glass opacity with fine mesh grid opacity in the middle and lower lobes of the right lung; most lesions were distributed in the field of the lung. After 6 days of hospitalization, the patient's condition deteriorated. Follow-up CT imaging (E–H) showed that the scope of the disease had considerably increased, such that diffuse GGO was observed, along with fine grid opacity and solid change opacity.